First Model Independent Separation of Multipole Form Factors in a Mixed Transition

P. E. Mueller,* C. N. Papanicolas,† and S. E. Williamson
Department of Physics and Nuclear Physics Laboratory, University of Illinois at Urbana-Champaign, Illinois 61801

A. Frey, A. Hecker, M. Korn, K. Merle, R. Nick, and H. Rothhaas
Institut für Kernphysik, Johannes Gutenberg Universität, Mainz, Germany
(Received 9 September 1998)

The magnitudes and relative phase of the $E2$ and $M1$ electron scattering form factors of the 6.32 MeV ($\frac{3}{2}^-$) state of ^{15}N have been measured at momentum transfers (q) of 0.63 and 1.07 fm^{-1}. These two transverse multipole form factors were separated using a combined analysis of single-arm (e, e') and coincident $(e, e'\gamma)$ data. This measurement is the first model independent separation of multipole form factors that contribute to a mixed transition.

PACS numbers: 25.30.Dh, 23.20.Js, 27.20.+n

The availability of high duty cycle electron beams has made coincident $(e, e'\gamma)$ electron scattering a valuable tool for the investigation of nuclear structure [1–3]. The experiment reported here measured the $(e, e'\gamma)$ cross section for the excitation of the 6.32 MeV ($\frac{3}{2}^-$) state of ^{15}N. It extends the use of the $(e, e'\gamma)$ reaction to the study of excitations of nonzero spin nuclei. In such nuclei a model independent separation of the multipole form factors contributing to the single-arm (e, e') cross section and subsequent reconstruction of transition charge and current densities is generally impossible. We demonstrate for the first time that such a separation can be performed with the measurement of an $(e, e'\gamma)$ cross section.

In cases where electron scattering yields individual multipole form factors the reconstruction of nuclear transition charge and current densities is feasible [4]. These experimentally determined densities provide detailed microscopic guidance to nuclear theory [5]. The (e, e') reaction allows the separation of only the incoherent sum of the longitudinal [$|F_L|^2 = \sum_\lambda F_L^\lambda(q)^2$] and transverse [$|F_T|^2 = \sum_\lambda F_T^\lambda(q)^2$] form factors. Therefore the individual multipole form factors, $F_{L,T}^\lambda(q)$, cannot in general be isolated except for zero spin nuclei and certain transitions in nonzero spin nuclei where spin and parity selection rules allow only one longitudinal and/or transverse multipole form factor. As a result, the reconstruction of transition charge and current densities has not been possible for important nonzero spin nuclei such as those adjacent to doubly closed shells.

The $(e, e'\gamma)$ reaction makes possible the separation of individual multipole form factors through the determination of the angular distribution of the deexcitation γ ray(s). The method is of general applicability, provided that one also considers the γ ray(s) produced in deexcitation to states other than the ground state, which will be the case in the study of higher ($\lambda \geq 3$) multipole form factors. In such cases the simultaneous detection of more than one of the γ rays of the resulting cascade will be highly advantageous. The form factor separation is achieved without the introduction of additional uncertainties in reaction dynamics since both the (e, e') and $(e, e'\gamma)$ reactions are entirely electromagnetic. A closely related and often complementary method is that of scattering electrons from polarized targets [6,7].

Because the coincident bremsstrahlung photon distribution is kinematically focused along the incident and scattered electron directions, the elastic radiative tail is significantly reduced for $(e, e'\gamma)$ cross section measurements where the photon is detected away from these two directions (typically in the backward scattering hemisphere). This is particularly important for the study of low lying states near the elastic peak and also for continuum states such as giant resonances which have a small photon decay probability. The bremsstrahlung coincidence cross section is less important in low Z nuclei such as ^{15}N [3], as is Coulomb distortion of the incident and scattered electron waves [8,9].

This first demonstration of multipole form factor separation was performed on an important transition in nuclear structure physics. The 6.32 MeV ($\frac{3}{2}^-$) state of ^{15}N has a simple shell model description as a proton hole excitation in the doubly closed ^{16}O core. As with other single particle (hole) states in odd-even nuclei adjacent to doubly closed shells, the 6.32 MeV ($\frac{3}{2}^-$) level is in a region of low excitation energy and low level density. The wide level spacing makes experimental investigation of this state possible. This is in contrast to stretched states, which also have a single particle (hole) nature but which are found in regions of high excitation energy and high level density [10].

This state has been extensively studied by single-arm (e, e') electron scattering [11–16]. Spin and parity selection rules allow the excitation of this state through a single longitudinal ($C2$) and two transverse multipoles ($E2$ and $M1$). As a result, measurements at different incident electron energies, E_e, and electron scattering angles, θ_e, for the same momentum transfer q (Rosenbluth method) can separate the longitudinal form factor consisting of only the F_{C2} multipole form factor ($F_{C2} = \pm\sqrt{|F_L|^2}$) from the

transverse form factor consisting of the incoherent sum of the F_{E2} and F_{M1} multipole form factors. Single-arm (e, e') electron scattering measurements of the transverse form factor are in disagreement with several theoretical calculations [11]. The $(e, e'\gamma)$ probe, by measuring the strength of each multipole form factor in states such as this, can help elucidate the significance of a number of effects that have been invoked to explain the observed significant departure from the shell model such as configuration mixing, core polarization, meson exchange currents, and partial occupancy. Furthermore, the technique presented here opens the way for the reconstruction of transition charge and current densities, which provide the most stringent test of the models that attempt to explain these effects.

A very accurate value of the photon point mixing ratio has been measured by photon scattering ($\rho = 0.137 \pm 0.005$) [17]. This quantity determines the real photon contribution to the angular variation of the $(e, e'\gamma)$ cross section. It also provides a measurement of F_{E2} and F_{M1} at the photon point.

The 6.32 MeV ($\frac{3}{2}^-$) level decays by photon emission to the ground state essentially 100% of the time [17]. Photon detector energy resolution requirements are relaxed because there is no need to discriminate between competing decays on the basis of photon energy.

The experiment was performed with the MAMI A electron accelerator at the Institut für Kernphysik, Johannes Gutenberg Universität, Mainz, Germany [18,19]. A 3–5 μA, 183.4 MeV continuous duty cycle electron beam bombarded a 45 mg/cm^2, 99.5% ^{15}N enriched melamine powder target pressed between two 8 μm CH_2 films. Scattered electrons were detected by a magnetic spectrometer and photons emitted from the target were detected by three coplanar NaI(Tl) scintillation detectors: a central $5'' \times 5''$ NaI(Tl) detector subtending 46.8 msr and two peripheral $3'' \times 3''$ NaI(Tl) detectors subtending 21.6 msr each and at $\pm 22.5°$ with respect to the central detector. The experimental apparatus is shown in Fig. 1.

Previous $(e, e'\gamma)$ experiments at Illinois using a similar electron spectrometer and photon detector array [2,3] showed that cross section measurements are prone to systematic error. By measuring ratios of $(e, e'\gamma)$ cross sections this systematic error can be substantially reduced [3]. Simultaneous cross section measurements with two (or more) photon detectors also eliminate the systematic error due to luminosity uncertainties and fluctuations. The additional systematic error introduced by different photon detector efficiencies can be reduced considerably by periodically interchanging the photon detectors. In this experiment, ratios of $(e, e'\gamma)$ cross sections were determined both with sequential cross section measurements using the single central photon detector and with simultaneous cross section measurements using the two peripheral photon detectors.

The energy resolution of this measurement is determined by the electron spectrometer. The detected photon is used only to tag the event. The electron excitation

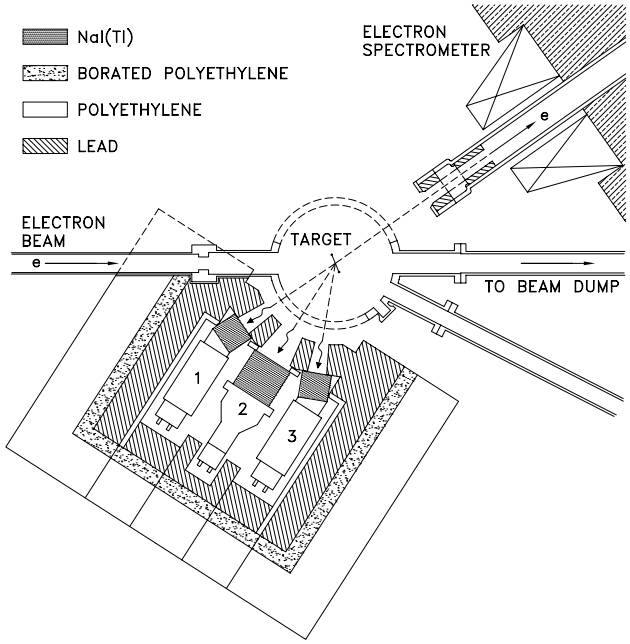

FIG. 1. Top view of the experimental apparatus used at Mainz for $(e, e'\gamma)$ measurements [23].

spectra were constructed by subtracting the electron momentum spectra of accidental coincidence events from the corresponding spectra of all electron-photon coincidence events. The $(e, e'\gamma)$ cross sections were extracted by fitting a line shape to the resulting excitation spectra as shown in Fig. 2. The line shape was a parametrization of the electron spectrometer response folded with calculations of

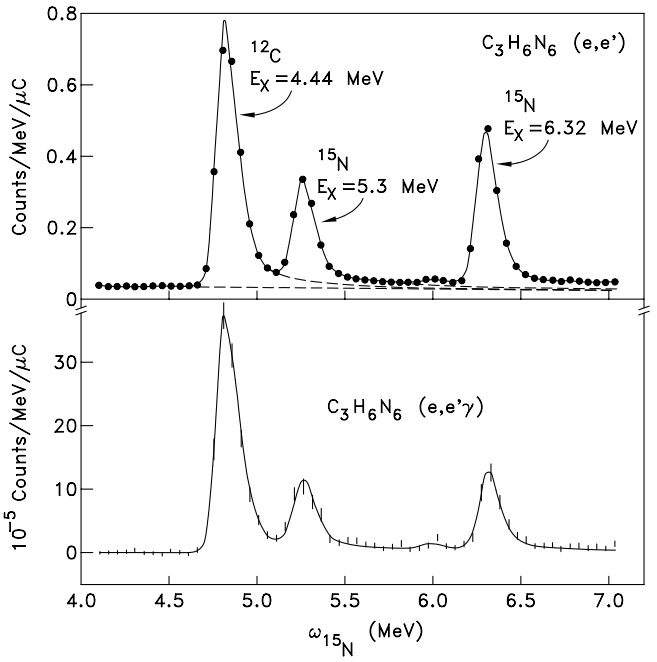

FIG. 2. Single-arm (e, e') (top) and coincident $(e, e'\gamma)$ (bottom) excitation energy ($\omega_{^{15}N}$) spectra for $E_e = 183.4$ MeV, $\theta_e = 72°$. Photons were detected with a $3'' \times 3''$ NaI(Tl) detector.

the various processes involved in the scattering of an electron from a nucleus and the passage of an electron through target material.

Because F_{C2} can be separated by the Rosenbluth method we need only to further separate F_{E2} and F_{M1}. The relationship $|F_T|^2 = |F_{E2}|^2 + |F_{M1}|^2$ can be rewritten in terms of form factor ratios:

$$\left(\frac{F_{E2}}{F_{C2}}\right)^2 + \left(\frac{F_{M1}}{F_{C2}}\right)^2 = \frac{|F_T|^2}{|F_L|^2}\,.$$

It also allows a mixing angle, β, to be defined such that

$$F_{E2} = F_T \sin\beta \quad \text{and} \quad F_{M1} = F_T \cos\beta\,.$$

The essence of our experiment is that, in addition to determining the magnitude of F_L and F_T, it measures the mixing angle β. The above equations imply that (e, e') measurements in the parameter space of F_{E2}/F_{C2} and F_{M1}/F_{C2} constrain the allowed solutions to a circle. Allowing for experimental uncertainties this implies a circular band. For $q = 1.07$ fm^{-1} ($E_e = 183.4$ MeV, $\theta_e = 72°$) our (e, e') measurements, along with previous (e, e') measurements [11], give the circular band shown in Fig. 3.

The ratio of two $(e, e'\gamma)$ cross sections for a $\frac{1}{2}^{\pm} \rightarrow \frac{3}{2}^{\pm}$ transition [7] measured at the same electron kinematics (E_e, θ_e) but at different photon emission angles $(\theta_\gamma, \phi_\gamma)$ yields a quadratic equation in F_{E2}/F_{C2} and F_{M1}/F_{C2}:

$$A\left(\frac{F_{E2}}{F_{C2}}\right)^2 + B\left(\frac{F_{M1}}{F_{C2}}\right)^2 + C\left(\frac{F_{E2}}{F_{C2}}\right)\left(\frac{F_{M1}}{F_{C2}}\right) + D\left(\frac{F_{E2}}{F_{C2}}\right) + E\left(\frac{F_{M1}}{F_{C2}}\right) + F = 0\,,$$

where A, B, C, D, E, and F are linear combinations of products of collimator-averaged photon angular functions, electron kinematic functions, the photon point mixing ratio ρ, and the measured cross section ratio. The constraint imposed by $(e, e'\gamma)$ as manifested in the preceding equation also has a simple geometric interpretation. It corresponds to a conic section in the parameter space of F_{E2}/F_{C2} and F_{M1}/F_{C2}. The experimentally determined band for $q = 1.07$ fm^{-1} is shown in Fig. 3 for a pair of photon emission angles. The simultaneous solution (fit) of these two equations gives F_{E2}/F_{C2} and F_{M1}/F_{C2} (or equivalently it determines the value of the mixing angle β). Multiple valued solutions are possible since two different quadratic curves (conic sections) can intersect at up to four points.

The extracted β values along with the corresponding photon point β value [17] are shown in Fig. 4. The normalized multipole form factors, F_{E2} and F_{M1}, are shown in Fig. 5. Two solutions are possible, indicated by filled and open symbols. The measurement at $q = 1.07$ fm^{-1} ($\theta_e = 72°$) is precise enough (the filled data circle is preferred) to eliminate this ambiguity by invoking Siegert's theorem [18]. Unfortunately, the ambiguity remains in the measurement at $q = 0.63$ fm^{-1} ($\theta_e = 40°$) due to large statistical uncertainty.

Also shown in Figs. 4 and 5 are the calculations of Suzuki [20]. These calculations, which are representative of the current level of sophistication in shell model calculations, are in good agreement with the data. The three curves exhibit the influence of core polarization (CP) and meson exchange currents (MEC) on the single particle (SP) result.

It is worth noting that the effects of fractional occupancy, which were not taken into account in the calculations of Figs. 4 and 5, cancel in leading order in the ratio of multipole form factors. In contrast, there is no cancelation for the extracted values of the individual F_{E2} and F_{M1} form factors. They tend to be lower than those calculated by Suzuki [20]. If the observed quenching from the full calculation is attributed to the effects of fractional occupancy our measurements at both values of q are consistent with a 70% partial occupancy of the $1p$ orbitals. Such a conclusion is in accord with a number of theoretical and

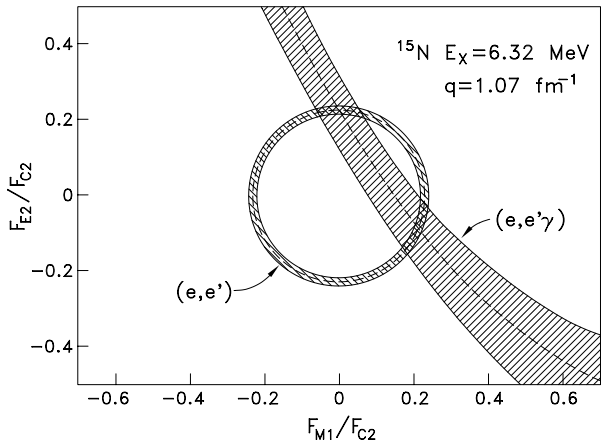

FIG. 3. Constraints imposed by the (e, e') and the $(e, e'\gamma)$ data. The nominal experimental values are depicted by dashed curves while the shaded areas indicate a 1σ statistical uncertainty.

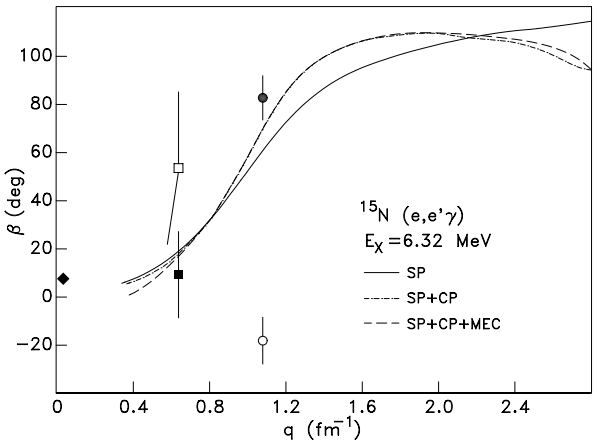

FIG. 4. The mixing angle β as a function of momentum transfer. The theoretical calculations are those of Suzuki [20].

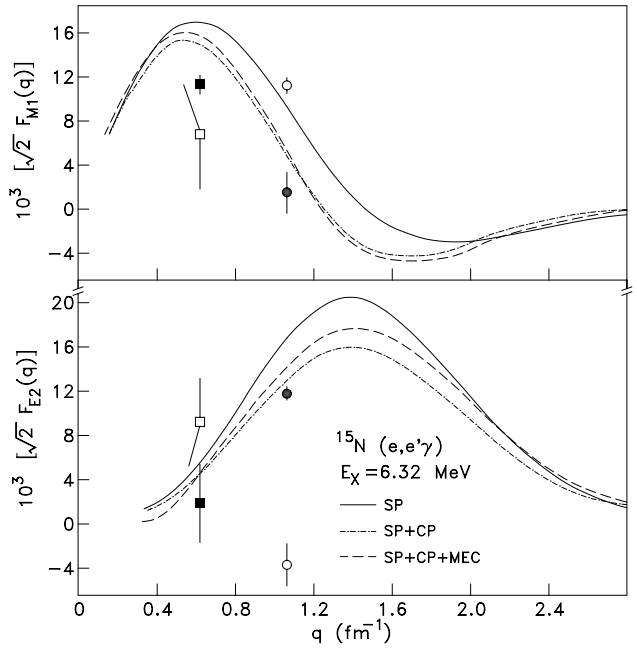

FIG. 5. The experimentally separated F_{E2} and F_{M1} form factors as a function of momentum transfer. The theoretical calculations are those of Suzuki [20].

experimental investigations on this issue [10,21,22]. Clearly data of higher statistical precision spanning a wider range of momentum transfer will be needed in order to conclusively confirm such a claim.

This work demonstrates that model independent separation of multipole form factors in mixed transitions can be accurately performed. The availability of high energy, high quality, high duty cycle electron beams at CEBAF, MAMI B, and MIT-Bates will allow similar separations to be efficiently performed over a wide range of momentum transfer, subject to the availability of the appropriate specialized detection equipment. Nuclear structure investigations using the accurate and interpretable results of inelastic electron scattering measurements can now be extended from zero spin nuclei to nonzero spin nuclei.

The authors are indebted to the MAMI accelerator staff for their help during data taking. We acknowledge valuable insight obtained as a result of discussions with L. S. Cardman, J. R. Deininger, T. W. Donnelly, E. A. J. M. Offermann, G. Ravenhall, and J. Wambach. This research was supported by the National Science Foundation under Grant No. NSF PHY86-10493 and the Deutsche Forschungsgemeinschaft.

*Present address: Oak Ridge National Laboratory, Oak Ridge, Tennessee 37831-6368.
†Present address: Physics Department, National and Capodistrian University of Athens, Athens, Greece.

[1] H. L. Acker and M. E. Rose, Ann. Phys. (N.Y.) **44**, 336 (1967).
[2] S. E. Williamson, Ph.D. thesis, University of Illinois, 1981.
[3] C. N. Papanicolas, S. E. Williamson, H. Rothhaas, G. O. Bolme, L. J. Koester, Jr., B. L. Miller, R. A. Miskimen, P. E. Mueller, and L. S. Cardman, Phys. Rev. Lett. **54**, 26 (1985).
[4] J. Heisenberg, Adv. Nucl. Phys. **12**, 61 (1981).
[5] B. Frois and C. N. Papanicolas, Annu. Rev. Nucl. Part. Sci. **37**, 133 (1987).
[6] T. W. Donnelly and A. S. Raskin, Ann. Phys. (N.Y.) **169**, 247 (1986).
[7] T. W. Donnelly, A. S. Raskin, and J. Dubach, Nucl. Phys. **A474**, 307 (1987).
[8] D. G. Ravenhall, R. L. Schult, J. Wambach, C. N. Papanicolas, and S. E. Williamson, Ann. Phys. (N.Y.) **178**, 187 (1987).
[9] I. Talwar, A. Hoque, and L. E. Wright, Phys. Rev. C **44**, 2694 (1991).
[10] C. N. Papanicolas, in *Nuclear Structure at High Spin, Excitation, and Momentum Transfer*, edited by Hermann Nann, AIP Conf. Proc. No. 142 (AIP, New York, 1986).
[11] R. P. Singhal, J. Dubach, R. S. Hicks, R. A. Lindgren, B. Parker, and G. A. Peterson, Phys. Rev. C **28**, 513 (1983).
[12] G. A. Beer, P. Brix, H.-G. Clerc, and B. Laube, Phys. Lett. **26B**, 506 (1968).
[13] E. B. Dally, M. G. Croissiaux, and B. Schweitz, Phys. Rev. C **2**, 2057 (1970).
[14] J. C. Kim, H. S. Caplan, and I. P. Auer, Phys. Lett. **56B**, 442 (1975).
[15] M. W. S. Macauley, R. P. Singhal, R. G. Arthur, S. W. Brain, W. A. Gillespie, A. Johnston, E. W. Lees, and A. G. Slight, J. Phys. G **3**, 1717 (1977).
[16] J. W. de Vries, Ph.D. thesis, University of Utrecht, 1987.
[17] R. Moreh and O. Shahal, Nucl. Phys. **A252**, 429 (1975).
[18] P. E. Mueller, Ph.D. thesis, University of Illinois, 1993.
[19] R. Nick, Diplomarbeit, Institut für Kernphysik, Johannes Gutenberg Universität, Mainz, 1988.
[20] T. Suzuki, Ph.D. thesis, University of Tokyo, 1978.
[21] V. R. Pandharipande, C. N. Papanicolas, and J. Wambach, Phys. Rev. Lett. **53**, 1133 (1984).
[22] L. Lapikás, Nucl. Phys. **A553**, 297c (1993).
[23] A. Hecker, Diplomarbeit, Institut für Kernphysik, Johannes Gutenberg Universität, Mainz, 1986.